Pis'ma v ZhETF, vol. 122, iss. 2, pp. 125 – 128

Comparison of spiral waves in simplified cardiac tissue models

S. Mohanty, D. Prusty, A. R. Nayak[1)]

International Institute of Information Technology (IIIT) Bhubaneswar, 751003 Bhubaneswar, India

Submitted 9 January 2025
Resubmitted 11 May 2025
Accepted 6 June 2025

Spiral waves of electrical activation in cardiac tissue can lead to life-threatening arrhythmias; therefore, understanding the mechanisms underlying the formation and propagation of these spiral waves is of great interest in cardiac dynamics. In this study, we conduct a comparative analysis of spiral waves using two simplified component models for cardiac tissue (a) the Panfilov model and (b) the Aliev–Panfilov model, by varying the parameters that govern excitability and recovery in both models. From our numerical studies, we observe states of (i) a periodic spiral, (ii) a quasi-periodic spiral, and (iii) spiral turbulence in both models, depending on the parameters. Our systematic study reveals that the Panfilov model exhibits conduction velocity restitution behavior and spiral transition sequences that closely resemble those observed in biophysical models; thus, it is better suited for studying wave dynamics in cardiac tissue compared to the Aliev–Panfilov model, providing an alternative to computationally expensive cardiac tissue models.

DOI: 10.31857/S0370274X25070206, EDN: QSJGES

Spiral wave patterns occur in a wide variety of chemical, physical, and biological systems. Prominent examples of biological systems include *Dictyostelium discoideum* amoebae aggregations [1], calcium waves in *Xenopus* oocytes [2], spreading depression in chicken retina [3], disinhibited mammalian neocortex [4], and electrical signaling in cardiac tissue [5]. However, spiral waves of electrical activation in cardiac tissue can disrupt the heart's normal rhythm, leading to life-threatening arrhythmias such as ventricular tachycardia (VT) and ventricular fibrillation (VF). It is generally accepted that a single rotating spiral is associated with VT, while its breakup into multiple spirals is linked to VF [5, 6]. Therefore, understanding the mechanisms underlying the formation and propagation of these spiral waves is of great interest in the field of cardiac dynamics. However, due to the inherent limitations of experimental studies, such as ethical considerations, costs, and uncontrollable variables, mathematical modeling remains essential for advancing our understanding of spiral wave dynamics and, consequently, cardiac arrhythmias.

In this paper, we employ two generic cardiac tissue models, the Panfilov model [7] and the Aliev–Panfilov model [8], to study and compare spiral wave dynamics in cardiac tissue. These simplified models consist of two variables: (a) the activation or fast variable, u, representing the activation process of the action potential, and (b) the recovery or slow variable, v, which describes the recovery process of the action potential.

The wave propagation in these models can be studied using the following Partial Differential Equations (PDEs):

$$\frac{\partial u}{\partial t} = D\nabla^2 u + f(u,v), \tag{1}$$

$$\frac{\partial v}{\partial t} = g(u,v), \tag{2}$$

where D is the diffusion coefficient. For the Panfilov model, the functions $f(u,v)$ and $g(u,v)$ are piecewise-linear in both u and v, and depend on other parameters; whereas, in the Aliev–Panfilov model, $f(u,v)$ is a cubic function of u and linear in v, and $g(u,v)$ is linear in both u and v.

Our study focuses on analyzing the impact of parameters, that controls the activation and recovery variables, in spiral wave patterns. For the Panfilov model, we vary ϵ_1 and ϵ_3 in the ranges $0.005 \le \epsilon_1 \le 0.05$ and $0.1 \le \epsilon_3 \le 2.0$ [9, 10], whereas for the Aliev–Panfilov model, the parameters a and μ_1 are varied within the ranges of $0.05 \le a \le 0.20$ and $0.05 \le \mu_1 \le 0.50$ [11, 12] to study and compare spiral waves.

For the Panfilov model, we set the spatial and temporal steps to 0.5 and 0.022, respectively. In the case of the Aliev–Panfilov model, these steps are adjusted to 0.6 (spatial) and 0.07 (temporal). To ensure consistent comparisons with biophysical ionic models, we adopt scaling factor from [9, 13] for dimensionless time and space steps by multiplying the dimensioned factors 5 ms and

[1)]e-mail: aloknayak@iiit-bh.ac.in

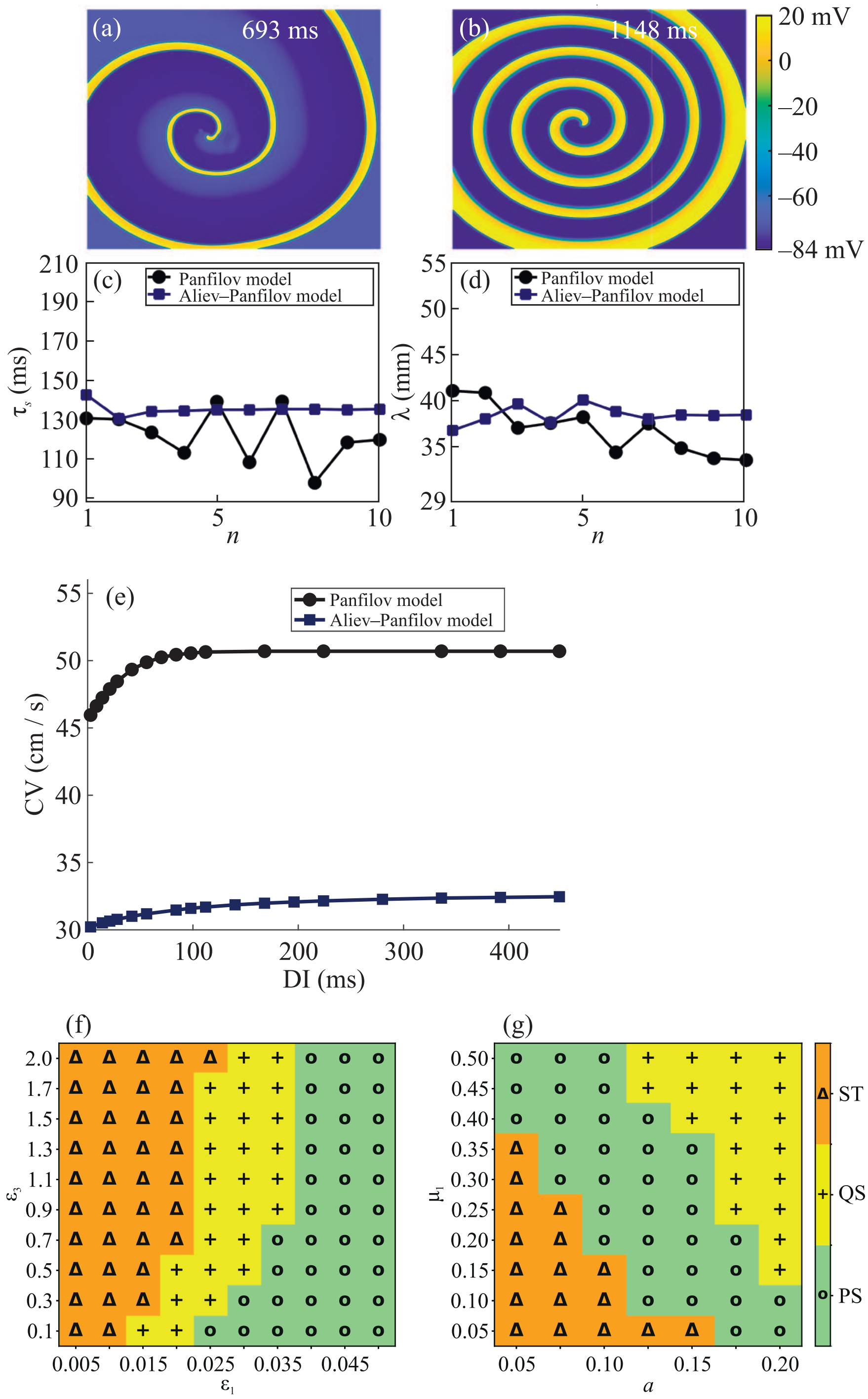

Fig. 1. (Color online) Pseudocolor plots of the transmembrane potential V_m showing a rotating spiral in (a) – the Panfilov model and (b) – the Aliev–Panfilov model, with model parameter settings; (c) – the rotation period τ of the spiral versus the spiral rotation number n; (d) – the wavelength λ of the spiral versus n; (e) – conduction velocity restitution (CVR) with model parameter settings; (f) – stability diagram of the spiral state in the ϵ_1–ϵ_3 parameter space for the Panfilov model; and (g) – stability diagram in the a–μ_1 parameter space for the Aliev–Panfilov model

1 mm for the Panfilov model, and 4 ms and 1 mm for the Aliev–Panfilov model. This scaling leads diffusion coefficient value $2\,\mathrm{cm}^2/\mathrm{s}$ and $2.5\,\mathrm{cm}^2/\mathrm{s}$ for the Panfilov and the Aliev–Panfilov models, respectively. With the above dimensioned spatial and temporal steps, we observe a single rotating spiral dominates in both models, for the

model parameter settings, as shown by the pseudocolor plots of V_m in Figs. 1a and b. However, the rotating spiral in the Panfilov model starts breaking from its core after $t \simeq 1.51$ s and eventually leads to spiral turbulence (ST), whereas the Aliev–Panfilov model maintains a stable core, resulting in a constant rotation period. From our numerical simulations, we find that the average rotation period of the rotating spiral, before it breaks, for the Panfilov model is $\tau_s \simeq 122$ ms, and 135 ms for the Aliev–Panfilov model, as depicted in Fig. 1c, consistent with the values reported in [9, 13]. Furthermore, we find the average wavelength of the rotating spiral λ_s values 36 mm and 39 mm for the Panfilov and the Aliev–Panfilov models, shown in Fig. 1d, agreeing with the reported values in [9, 13].

In Figure 1e, we show conduction velocity restitution (CVR) plots of both Panfilov and Aliev–Panfilov models with model parameter settings. This numerical framework allows us to explore how changes in pacing cycle length (PCL) or diastolic interval (DI), related by PCL = APD + DI with APD representing action potential duration, impact the propagation of electrical signals and subsequently influence spiral wave patterns in cardiac tissue. In the Panfilov model, the initial segment of the CVR curve exhibits a steep incline, a characteristic of wave instability [6, 14], resulting in ST in the two-dimensional domain (see, Fig. 1a for pre-breakup). However, the CVR curve initial segment does not increase steeply for the Aliev–Panfilov model, and therefore, a stable rotating spiral in the domain shown in Fig. 1b. Our results yield a CV of 50.7 cm/s for the Panfilov model and 32.4 cm/s for the Aliev–Panfilov model.

In Figures 1f and g, we present the stability diagrams of the spiral states in the ϵ_1–ϵ_3 parameter space for the Panfilov model and in the a–μ_1 parameter space for the Aliev–Panfilov model, respectively; the colors with symbols (brown, △), (yellow,+) and (green,○) represent the ST, quasi-periodic spiral (QS) and periodic spiral (PS) states, respectively. The stability diagram of the Panfilov model reveals that low and high values of ϵ_1 result in ST and PS states, respectively, whereas intermediate values of ϵ_1 lead to the QS state. In particular, for a given ϵ_3 value, increasing ϵ_1 induces a transition from ST to PS state through intermediate QS state. However, for $\epsilon_3 > 0.9$, the transition boundaries remain nearly unchanged, whereas $\epsilon_3 < 0.9$, the transition boundaries shift towards the left, as ϵ_1 varies. When ϵ_3 varies, the transition from the spiral state ST to PS depends on the values of ϵ_1. In particular, $\epsilon_1 < 0.015$ or $\epsilon_1 > 0.035$ lead to the ST or the PS states, respectively, without transitioning to other spiral states, despite increasing ϵ_3 values. However, for $0.015 < \epsilon_1 < 0.035$, decreasing ϵ_3 results in one of the following transitions: (i) ST to QS state, (ii) ST to PS state via the QS state, or (iii) QS to PS state. In the Aliev–Panfilov model, for low values of a (< 0.10) or μ_1 (< 0.10), increasing μ_1 (or a) results in a transition from the ST state to the PS state. In contrast, for high values of a (> 0.175) or μ_1 (> 0.40), a transition from the PS state to the QS state occurs as μ_1 (or a) is increased. In the intermediate range of $0.10 < a < 0.175$ (or $0.10 < \mu_1 < 0.40$), the ST state transitions to the PS state via the QS state as μ_1 (or a) increases. These observations from the stability diagram also illustrate the shifting stability regimes of the ST, QS, and PS spiral states within the $a - \mu_1$ parameter space.

We obtained three major spiral states, namely, PS, QS and ST, from the numerical studies of both Panfilov and Aliev–Panfilov models, depending on the values of (ϵ_1, ϵ_3) and (a, μ_1) parameters. From the Panfilov model, we observed that, as we decrease the parameter ϵ_1 values, a PS state transitions to an ST state with an intermediate QS state, agreeing with the results obtained in complex biophysical cardiac models [15, 16]. However, our studies on the Aliev–Panfilov model revealed that increasing the parameter a values leads to an ST state to a QS state through a PS state (Fig. 1g); such transitions have never been observed in cardiac tissue models. We also noticed from the spiral state stability diagrams, shown in Fig. 1f, that the parameter ϵ_3 values do not significantly influence the spiral state transition boundaries compared to ϵ_1 values in the Panfilov model, whereas in the Aliev–Panfilov model, the parameter μ_1 has the same effect as the parameter a.

Our systematic study reveals that the Panfilov model exhibits CVR behavior and spiral transition sequences that closely resemble those observed in biophysical models; thus, it is better suited for studying wave dynamics in cardiac tissue compared to the Aliev–Panfilov model, providing an alternative to computationally expensive cardiac tissue models.

We thank the International Institute of Information Technology (IIIT), Bhubaneswar, India, for their computational resources and support.

Funding. Dr. Alok Ranjan Nayak acknowledges support from Odisha State Higher Education Council (OSHEC) through grant 22SF/PH/089.

Conflict of interest. The authors of this work declare that they have no conflicts of interest.

1. S. Sawai, P. A. Thomason, and E. C. Cox, Nature **433**, 323 (2005).
2. J. Lechleiter, S. Girard, E. Peralta, and D. Clapham, Science **252**, 123 (1991).

3. Y. Yu, L. M. Santos, L. A. Mattiace, M. L. Costa, L. C. Ferreira, K. Benabou, A. H. Kim, J. Abrahams, M. V. Bennett, and R. Rozental, Proceedings of the National Academy of Sciences **109**, 2585 (2012).
4. X. Huang, W. C. Troy, Q. Yang, H. Ma, C. R. Laing, S. J. Schiff, and J.-Y. Wu, J. Neurosci. **24**, 9897 (2004).
5. S. Alonso, M. Bär, and B. Echebarria, Reports on Progress in Physics **79**, 096601 (2016).
6. F. H. Fenton, E. M. Cherry, H. M. Hastings, and S. J. Evans, Chaos: An Interdisciplinary Journal of Nonlinear Science **12**, 852 (2002).
7. A. Panfilov and P. Hogeweg, Phys. Lett. A **176**, 295 (1993).
8. R. R. Aliev and A. V. Panfilov, Chaos, Solitons & Fractals **7**, 293 (1996).
9. A. V. Panfilov, Chaos: An Interdisciplinary Journal of Nonlinear Science **8**, 57 (1998).
10. T. Shajahan, S. Sinha, and R. Pandit, Int. J. Mod. Phys. B **17**, 5645 (2003).
11. A. Panfilov, Phys. Rev. Lett. **88**, 118101 (2002).
12. K. H. ten Tusscher and A. V. Panfilov, Multiscale Modeling & Simulation **3**, 265 (2005).
13. A. Panfilov, S. C. Müller, V. S. Zykov, and J. P. Keener, Phys. Rev. E **61**, 4644 (2000).
14. Z. Qu, F. Xie, A. Garfinkel, and J. N. Weiss, Annals of Biomedical Engineering **28**, 755 (2000).
15. T. Shajahan, A. R. Nayak, and R. Pandit, PLoS One **4**, e4738 (2009).
16. K. Rajany, A. R. Nayak, R. Majumder, and R. Pandit, Physics Open **13**, 100120 (2022).